# Second harmonic generation with focused beams in a pair of walkoff-compensating crystals

Michael V. Pack[a], Darrell J. Armstrong[a], Arlee V. Smith[a,*], Michael E. Amiet[b]

[a] *Dept. 1118, Sandia National Laboratories, Albuquerque, NM 87185-1423, USA*
[b] *Physics Department, Duke University, Durham, NC 27708, USA*

## Abstract

We develop the heuristic theory of second harmonic generation with focused beams in walkoff-compensating crystals, and compare it with experiments, demonstrating excellent agreement.
© 2003 Elsevier Science B.V. All rights reserved.

## 1. Introduction

The efficiency of frequency conversion via parametric mixing in nonlinear crystals is often limited by birefringent walkoff. Considerable prior work has focused on the use of two crystals oriented to compensate spatial walkoff [1–5] in order to achieve better efficiency and larger acceptance angles. In a previous paper we presented calculations and experiments that indicated increased tolerance to beam tilt as well as increased second harmonic (SH) conversion efficiency as benefits of walkoff compensation [1]. Our calculations included both plane wave and focused beam cases but our experiments covered only plane waves. Other papers have presented theory and measurements that appeared to contradict our predictions for focused beams [3]. In this paper we present laboratory measurements for focused beams that verify our earlier predictions. We first present new plane wave calculations and measurements to illustrate our methods and also to measure the intercrystal phase shift due to the anti reflective dielectric coatings on our crystals. We then apply the same calculation methods to focused beams, using the measured intercrystal phase shift, and compare our calculations with our measurements. We compare both the conversion efficiency and the far-field second harmonic beam profiles, achieving excellent agreement.

---

\* Corresponding author. Tel.: +5058445810; fax: +5058445459.
*E-mail addresses:* mvpack@sandia.gov (M.V. Pack), arlsmit@sandia.gov (A.V. Smith).

## 2. Plane waves

### 2.1. Plane wave theory

In this section we present equations for SH conversion efficiency using two identical crystals with either the same or opposite signs of $d_{\mathrm{eff}}$, in the undepleted-pump, plane wave approximation. These equations predict improvements in the tilt tolerance for the fundamental beam, and in the conversion efficiency, when two crystals are arranged for walkoff compensation with the same sign of $d_{\mathrm{eff}}$.

When the beam waist is much larger than the lateral displacement due to walkoff ($w_0 \gg \rho L$), and the Raleigh length is much greater than the crystal length ($z_0 \gg L$), the fundamental and harmonic waves can be treated as plane waves. The heuristic method of Boyd and Kleinman [6] consists of dividing the crystal into infinitesimally thin slices in the $z$, or propagation, direction and summing the harmonic waves radiated by each of the d$z$ slices. For two crystals arranged as shown in Fig. 1 this summation is expressed by the integral

$$\varepsilon_{2\omega} = \frac{2\mathrm{i}\omega d_{\mathrm{eff}}\varepsilon_\omega^2}{n_{2\omega}c}\left\{\int_{-(L+D)}^{-D}\mathrm{d}z\,\mathrm{e}^{-\mathrm{i}\Delta k_1(z+D)} + \mathrm{e}^{-\mathrm{i}\Delta\phi}\int_D^{(L+D)}\mathrm{d}z\,\mathrm{e}^{-\mathrm{i}\Delta k_2(z-D)}\right\}, \tag{1}$$

where $\varepsilon_\omega$ and $\varepsilon_{2\omega}$ are the fundamental and SH electric fields, $\Delta k = k_{2\omega} - 2k_\omega$, and $d_{\mathrm{eff}}$ is the effective second-order nonlinearity of the crystals. The phase term $\Delta\phi$ multiplying the second integral is the intercrystal phase shift between the harmonic and fundamental waves introduced by the antireflection (AR) coatings and by the dispersion of air. The AR coatings on our crystals are identical, so we write the phase shift as

$$\Delta\phi = 2\phi_{\mathrm{AR}} + 2D\Delta k_{\mathrm{air}}, \tag{2}$$

where $\phi_{\mathrm{AR}}$ is the phase difference ($\phi_{2\omega} - 2\phi_\omega$) due to a single AR coating, and the phase difference due to propagation through a distance $2D$ in air is $2D\Delta k_{\mathrm{air}} = 4Dk_0(n_{2\omega} - n_\omega)$, with $k_0 = \omega/c$. Note that the phase of the first integrand, evaluated at $z = -D$, and the phase of the second integrand, evaluated at $z = D$, differ by $\Delta\phi$, which is exactly the phase difference accumulated after leaving the first crystal and before entering the second crystal. We emphasize this point because in Section 3.1 we will repeat this calculation for lowest order Gaussian beams using the same arguments presented here. The phase difference between integrals is a point of disagreement between Feve et al. [3] and results we will derive in Section 3.1 which agree with Zondy [2] and Smith et al. [1].

Performing the integration of Eq. (1) and using $I = |\varepsilon|^2 n\varepsilon_0 c/2$ yields the irradiance of the SH

$$I_{2\omega} = \frac{2\omega^2 d_{\mathrm{eff}}^2 L^2 I_\omega^{(\mathrm{Total})2}}{\varepsilon_0 c^3 n_{2\omega} n_\omega^2}\left\{\mathrm{sinc}^2\left(\frac{\Delta k_1 L}{2}\right) + \mathrm{sinc}^2\left(\frac{\Delta k_2 L}{2}\right) + 2\mathrm{sinc}\left(\frac{\Delta k_1 L}{2}\right)\mathrm{sinc}\left(\frac{\Delta k_2 L}{2}\right)\right.$$
$$\left. \times \cos\left(\Delta\phi + \frac{L(\Delta k_1 + \Delta k_2)}{2}\right)\right\}. \tag{3}$$
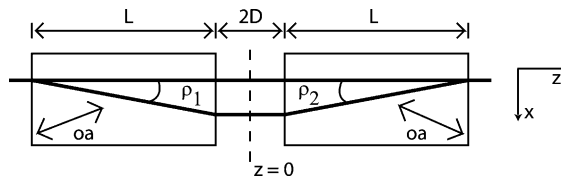


Fig. 1. Diagram of two negative uniaxial crystals arranged for walkoff-compensated SH generation. The arrows labeled 'oa' indicate the orientation of the optic axis. Walkoff compensation corresponds to $\rho_1 = \rho_2$.

Note that reversing the sign of $d_{\text{eff}}$ in the second crystal reverses the sign of the second integral. This is equivalent to adding $\pi$ to $\Delta\phi$, which also reverses the sign of the second integral. In the remainder of this paper we will use the same sign for the two $d_{\text{eff}}$'s and account for sign reversals by adding $\pi$ to $\Delta\phi$.

If the two crystals are first aligned so $\Delta k_1 = \Delta k_2 = 0$ and the fundamental beam is then tilted away from the phase matching angle, the phase mismatches are related by $\Delta k_1 = -\Delta k_2$. In this case, if $\phi = 0$, Eq. (3) reduces to

$$I_{2\omega} = \frac{2\omega^2 d_{\text{eff}}^2 L^2 I_{\omega}^{(\text{Total})2}}{\varepsilon_0 c^3 n_{2\omega} n_{\omega}^2} 4\text{sinc}^2\left(\frac{\Delta k_1 L}{2}\right) \tag{4}$$

in agreement with Eq. (16) of [1], and Eq. (1) of [2]. This equation indicates a doubled tilt tolerance for two walkoff-compensating crystals compared with a single crystal of length $2L$ for which the SH is proportional to $\text{sinc}^2(\Delta kL)$. This is at odds with the claim of Feve et al. [3] where it is stated in Eqs. (3.1)–(3.4) that the dependence is $\text{sinc}^2(\Delta kL/2)\cos^2(\Delta kL)$, indicating a reduced, rather than increased, tilt tolerance relative to a single crystal of length $2L$ due to the $\cos^2(\Delta kL)$ term.

## 2.2. Plane wave experiment

We performed laboratory measurements to verify the plane wave theory and to establish the intercrystal phase shift, $\Delta\phi$, for our crystals. In Fig. 1 we show two crystals arranged for walkoff compensation. The walkoff direction of the extraordinary polarized SH beam is opposite in the two crystals. In our experiments the two crystals are identical, 7.08 mm long BBO crystals cut for type I phase matching at $\theta = 23°$. It is possible to reverse the sign of $d_{\text{eff}}$ in the second crystal without reversing its walkoff direction by rotating it 180° about an axis normal to the page [4]. We compare these two cases.

Our experiments consist of recording the SH conversion efficiency as we vary the values of $\Delta k_1$ and $\Delta k_2$ by rotating the crystals individually by small amounts about axes normal to the page. The experimental apparatus is diagrammed in Fig. 2. The source of fundamental light is a single-longitudinal-mode Nd:YAG laser that produces 10 ns pulses at a repetition rate of 10 Hz. We spatially filtered the 1064 nm fundamental beam by focusing it through a 225 μm diameter wire die. The transmitted beam was collimated and the resultant Airy pattern was truncated at the first Airy null to create a nearly Gaussian beam of 1.5 mm diameter. The walkoff angle for our crystals is $\rho = 55.7$ mrad, which gives a displacement of 0.394 mm in each crystal, much less than the fundamental beam diameter. We use a polarizer and half-wave plate to adjust the fundamental power to limit the fundamental depletion to less than 2%. Depletion is monitored by comparing the signals from the 1064 nm detectors before and after the crystal. The crystals were rotated on mounts with 75.4 μrad. angular resolution, which corresponds to 47.5 μrad. internal angle resolution. This step size corresponds to a change in $\Delta kL$ of $0.112\pi$ rad $= 0.366$ rad for our crystals. The crystals are separated by 2 mm unless otherwise noted.

The baseline signals at each $(\Delta k_1, \Delta k_2)$ is measured by averaging over 5 pulses with the shutter closed. The normalized SH conversion efficiency $\eta(\Delta k_1, \Delta k_2)$ is determined by averaging the quotient of the baseline-subtracted harmonic signal and the square of the baseline-subtracted fundamental signal over 5 pulses. Each conversion surface is normalized to its peak value for ease of comparison.

The measured harmonic conversion efficiency, $\eta(\Delta k_1, \Delta k_2)$, is displayed in Fig. 3 along with a surface calculated using Eq. (3). The intercrystal phase shift, $\Delta\phi$, was adjusted in the calculation to give the best agreement with the measured surface. The best fit is for $\Delta\phi = -152°$. The ratio of heights of the two central peaks of $\eta(\Delta k_1, \Delta k_2)$ is quite sensitive to $\Delta\phi$, so our measurement error for $\Delta\phi$ is only $\pm 2°$. We also measured $\Delta\phi$ after reorienting the second crystal to reverse the sign of its $d_{\text{eff}}$, but this resulted in a surface with a single peak located near $(\Delta k_1, \Delta k_2) = (0, 0)$ and the value of $\Delta\phi$ had a higher uncertainty. As a check of our value of $\Delta\phi$ we increased the crystal separation to 11 mm and found a best fit with $\Delta\phi = -125°$.
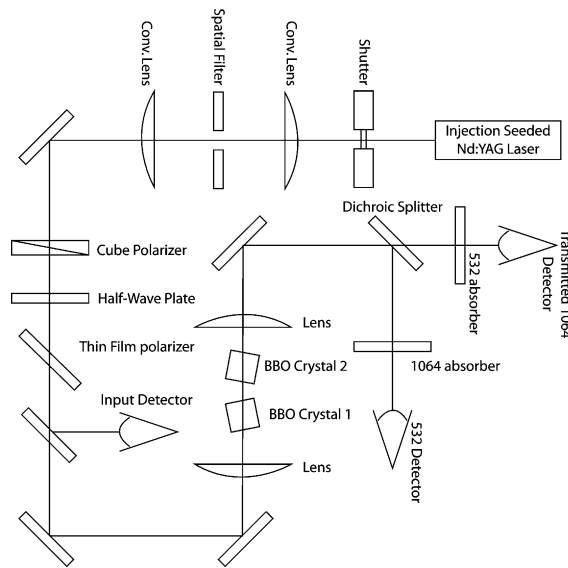
Fig. 2. Diagram of the measurement apparatus. The 1064 nm fundamental is from an injection-seeded, Q-switched Nd:YAG laser and has a pulse duration of 10 ns FWHM. The spatially filtered 1064 nm beam was o-polarized. Its energy was adjusted for negligible fundamental depletion by rotating the half-wave plate. For the focused beam measurements the focal waist lay midway between the crystals.
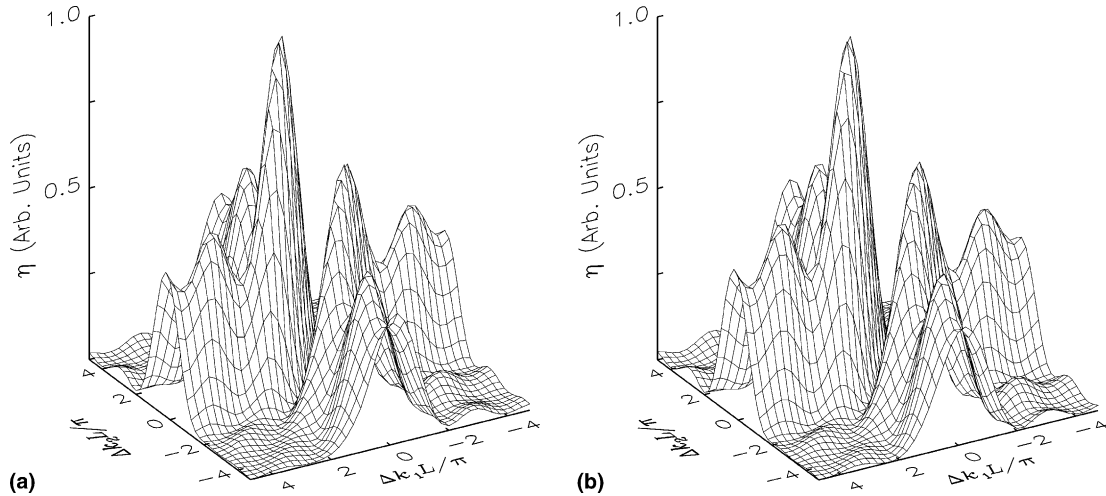


Fig. 3. Surfaces of $\eta(\Delta k_1, \Delta k_2)$, or SH efficiency versus $\Delta k_1$ and $\Delta k_2$, (a) measured and (b) calculated for plane waves according to Eq. (3). We found that using an intercrystal phase shift (due to crystal AR coatings and air – see text for details) of $\Delta\phi = -152°$ for the calculated surface gave the best match to the measured surface.

From this we deduce $\Delta k_{\mathrm{air}} = 3°/\mathrm{mm}$, compared with $\Delta k_{\mathrm{air}} = 2.9°/\mathrm{mm}$ expected [7] for 20 °C dry air at the local atmospheric pressure of 87 kPa.

If we assume the second crystal was oriented so the $d_{\mathrm{eff}}$'s for the two crystals had opposite signs in the case where $\Delta\phi = -152°$, the measured phase shift due to air and coatings is $+28°$. Of this, the 2 mm of air

between crystals accounts for 6°, so the two identical AR coatings on the inner faces of the crystals must have a total phase shift of +22°, or +11° apiece. The manufacturer predicted a phase shift of −13° ± 25° per coating, consistent with our measured value. This measured value of the phase shift due to the crystal coatings will be used in our subsequent analyses.

## 3. Focused beams

### 3.1. Focused beam theory

For focused beams we again use the heuristic integration method, summing the SH contributions from the d$z$ slices. It has been shown that for Gaussian beams the heuristic method gives the same result as the more formal method of Green's functions [6,8]. Refs. [1–3] also derived their respective results using the heuristic method of Boyd and Kleinman.

We will treat both type I and type II processes starting with type I. For a focused Gaussian fundamental beam the SH polarization in each d$z$ slice is Gaussian in transverse profile with the same radius of curvature as the local fundamental beam. The radiated harmonic field from each slice is also a Gaussian beam with the same waist location as the fundamental, and with the same Rayleigh range $z_0$, but with a waist smaller by $\sqrt{2}$. For a fundamental beam described by

$$\varepsilon_\omega(x',y',z') = \frac{\varepsilon_0}{(1+i\tau')}\exp\left[-\frac{x'^2+y'^2}{w_0^2(1+i\tau')}\right], \tag{5}$$

where $w_0$ is the beam waist, $z_0 = k_\omega w_0^2/2$, and $\tau' = z'/z_0$, the harmonic field radiated by a slice of thickness d$z$ is

$$\varepsilon_{2\omega}(x',y',z') = dz\frac{2i\omega}{n_{2\omega}c}d_{eff}\frac{\varepsilon_0^2}{(1+i\tau')^2}\exp\left[-2\frac{x'^2+y'^2}{w_0^2(1+i\tau')}\right]. \tag{6}$$

The beams diffract more rapidly in the air gap than they would over the same length inside the crystals. However, for simplicity we treat the beams as though they are always inside a medium with refractive index of the crystals, $n_\omega = n_{2\omega}$. To account for this, the $D$ appearing in the following analysis is half the physical length of the air gap multiplied by $n_\omega$ rather than half the air gap. The value of $\Delta\phi$ remains the same as for plane waves.

In propagating from location $z'$ to the end of the second crystal the e-polarized harmonic field will experience lateral walkoff in the $x$ direction due to birefringence. To relate the position $x$ in a plane located downstream from the crystals to the position $x'$ inside the crystals we use the transformation

$$
\begin{aligned}
x' &= x - \rho_i(D - |z'|), \\
y' &= y,
\end{aligned} \tag{7}
$$

where $\rho_1$ is the walkoff angle in the first crystal and $\rho_2$ is the walkoff angle in the second crystal. If the fundamental waist is midway between the crystals, the harmonic field in the target plane at $z$ is given by

$$
\begin{aligned}
\varepsilon_{2\omega}(x,y,z) = \frac{2i\omega\varepsilon_0^2 z_0 d_{eff}}{n_{2\omega}c(1+i\tau)}\Bigg\{ &\int_{-L+D/z_0}^{-D/z_0} d\tau'\frac{e^{-i\Delta k_1 z_0(\tau'+D/z_0)}}{1+i\tau'}\exp\left(-2\frac{\left[x-\rho_1(D+z_0\tau')\right]^2+y^2}{w_0^2(1+i\tau)}\right) \\
&+ e^{-i\Delta\phi}\int_{D/z_0}^{L+D/z_0} d\tau'\frac{e^{-i\Delta k_2 z_0(\tau'-D/z_0)}}{1+i\tau'}\exp\left(-2\frac{\left[(x-\rho_2(D-z_0\tau')\right]^2+y^2}{w_0^2(1+i\tau)}\right)\Bigg\},
\end{aligned} \tag{8}
$$

where $\tau = z/z_0$, and $\Delta\phi$ is the intercrystal phase shift. By setting $\rho_1 = \rho_2$ Eq. (8) describes walkoff-compensated doubling where both crystals have the same sign for $d_{\text{eff}}$. For a nonwalkoff-compensated orientation we would use $\rho_1 = -\rho_2$, and if $d_{\text{eff}}$ were opposite in the two crystals we would add $\pi$ to $\Delta\phi$.

We emphasize that in Eq. (8) the phase difference between the innermost faces of the crystals (i.e., the crystal faces corresponding to the first integrand evaluated at $\tau' = D/z_0$, and the second integrand evaluated at $\tau' = D/z_0$) is correct. The phase difference is $[\Delta\phi + 2\arctan(D/z_0)]$, where $\Delta\phi$ is given by Eq. (2), and the arctan term is the Guoy, or focal, phase shift. For type I SH generation in optically contacted, walkoff-compensated, and lossless crystals $D = 0$, $\rho_1 = \rho_2$, and $\Delta\phi = 0$, in which case Eq. (8) is identical with Eqs. (3.1)–(3.4) in [3], except Feve's result has an intercrystal phase difference of $[L(\Delta k_1 - \Delta k_2)]$. Clearly, for optically contacted crystals the intercrystal phase difference should be zero.

The SH power can be calculated by taking the target plane to the far field ($\tau \to \infty$), multiplying Eq. (8) by its complex conjugate, and integrating over the transverse coordinates $x$ and $y$. This gives

$$\mathscr{P}_{2\omega} = \frac{2\omega^3 \mathscr{P}_\omega^{(\text{Total})^2} L d_{\text{eff}}^2}{\pi\varepsilon_0 c^4 n_\omega^2} h_{\text{I}}(\Delta k_1, \Delta k_2, \beta_1, \beta_2, L, z_0), \tag{9}$$

where $\beta_i = \rho_i z_0 / w_0$, and $h_{\text{I}}(\Delta k_1, \Delta k_2, \beta, L, z_0)$ is

$$
\begin{aligned}
h_{\text{I}}(\Delta k_1, \Delta k_2, \beta, L, z_0) = {} & \frac{z_0}{2L} \int \int_{D/z_0}^{L+D/z_0} \mathrm{d}\tau' \mathrm{d}\tau'' \frac{1}{(1+\tau'^2)(1+\tau''2)} \left[ \mathrm{e}^{-\beta_1^2(\tau'-\tau'')^2} \left\{ (1+\tau'\tau'') \cos\left(z_0 \Delta k_1(\tau'-\tau'')\right) \right. \right. \\
& \left. - (\tau'-\tau'') \sin\left(z_0 \Delta k_1(\tau'-\tau'')\right) \right\} + \mathrm{e}^{-\beta_2^2(\tau'-\tau'')^2} \left\{ (1+\tau'\tau'') \cos\left(z_0 \Delta k_2(\tau'-\tau'')\right) \right. \\
& \left. - (\tau'-\tau'') \sin\left(z_0 \Delta k_2(\tau'-\tau'')\right) \right\} + 2\mathrm{e}^{-(\beta_1\tau'-\beta_2\tau''+c_1)^2} \left\{ (1-\tau'\tau'') \cos\left(z_0(\Delta k_1\tau' \right.\right. \\
& \left. + \Delta k_2\tau'') + \Delta\phi - D(\Delta k_1 + \Delta k_2)\right) - 2(\tau'+\tau'') \sin\left(z_0(\Delta k_1\tau' + \Delta k_2\tau'') + \Delta\phi \right. \\
& \left.\left.\left. - D(\Delta k_1 + \Delta k_2)\right)\right\} \right]
\end{aligned}
\tag{10}
$$

with $c_1 = D(\rho_1 - \rho_2)$. Similar expressions for the walkoff-compensated case ($\rho_1 = \rho_2$) can be found in Eqs. (27)–(30) of [1] and in Eqs. (4a)–(4c) of [2].

For type II doubling the fundamental waves have opposite polarizations so one walks off relative to the other, while the SH walkoff is the same as one of the fundamental beams. The SH polarization in the overlap region between the fundamental beams is still circular with the same properties as in type I doubling except it becomes progressively weaker as the fundamental beams separate. Using the same arguments as for type I SH conversion above, the $h$ for type II SH conversion in the walkoff-compensated case is changed to

$$
\begin{aligned}
h_{\text{II}}(\Delta k_1, \Delta k_2, \beta, L, z_0) = {} & \frac{z_0}{2L} \int \int_{D/z_0}^{L+D/z_0} \mathrm{d}\tau' \mathrm{d}\tau'' \frac{\mathrm{e}^{-\frac{\beta^2}{4}(\tau'-\tau'')^2 - \alpha(\tau',\tau'',c')}}{(1+\tau'^2)(1+\tau''2)} \left[ \left\{ (1+\tau'\tau'') \cos\left(z_0\Delta k_1(\tau'-\tau'') \right.\right.\right. \\
& \left. + \Phi_-(\tau',\tau'',c')\right) - (\tau'-\tau'') \sin\left(z_0\Delta k_1(\tau'-\tau'') + \Phi_-(\tau',\tau'',c')\right) \right\} \left\{ (1+\tau'\tau'') \right. \\
& \times \cos\left(z_0\Delta k_2(\tau'-\tau'') + \Phi_-(\tau',\tau'',c')\right) - (\tau'-\tau'') \sin\left(z_0\Delta k_2(\tau'-\tau'') \right. \\
& \left. + \Phi_-(\tau',\tau'',c')\right) \right\} + 2\left\{ (1-\tau'\tau'') \cos\left(z_0(\Delta k_1\tau' + \Delta k_2\tau'') + \Delta\phi - D(\Delta k_1 + \Delta k_2) \right.\right. \\
& \left. - \Phi_+(\tau',\tau'',c')\right) - (\tau'+\tau'') \sin\left(z_0(\Delta k_1\tau' + \Delta k_2\tau'') + \Delta\phi - D(\Delta k_1 + \Delta k_2) \right. \\
& \left.\left.\left. - \Phi_+(\tau',\tau'',c')\right)\right\} \right],
\end{aligned}
\tag{11}
$$

where

$$\Phi_\pm(\tau',\tau'',c') = \frac{\tau''(\tau''\beta - c')^2}{2(1+\tau''2)} \pm \frac{\tau'(\tau'\beta - c')^2}{2(1+\tau'^2)},$$

$$\alpha(\tau', \tau'', c') = \frac{(\tau''\beta - c')^2}{2(1 + \tau''2)} + \frac{(\tau'\beta - c')^2}{2(1 + \tau'^2)},$$

and

$$c' = \rho(L + D)/w_0.$$

We have assumed equal power in the two fundamental waves. This can be used in place of $h_I$ in Eq. (9) to find the SH power. In the limit of weak focusing ($\tau', \tau'' \ll 1$), $\Phi_\pm = 0$ and this expression reduces to Eqs. (3.1)–(3.4) of [3] except for the phase terms $\exp(-i\Delta k_2 L/2)$ and $\exp(-i\Delta k_1 L/2)$ that appear in Eq. (3.4) of [3].

Both of the derivations above assumed a CW fundamental beam. For a pulsed source with a Gaussian time profile, we let $\varepsilon_\omega \rightarrow \varepsilon_\omega \exp(-t^2/\sigma_t^2)$. In Eq. (9) we make the substitutions

$$U_\omega = \mathscr{P}_\omega \sigma_t \sqrt{\pi/2}$$

and

$$U_{2\omega} = \mathscr{P}_{2\omega} \sigma_t \sqrt{\pi}/2.$$

The efficiency of SH conversion for a Gaussian pulse is

$$\eta = \frac{\mathscr{P}_{2\omega}}{\mathscr{P}_\omega^{(\text{Total})} \sigma_t \sqrt{\pi}}. \tag{12}$$

### 3.2. Focused beam measurement

We numerically evaluated $h_I(\Delta k_1, \Delta k_2, \beta, L, z_0)$ using the appropriate values for our BBO crystals and our experimental conditions of a 60 μm focal waist located midway between the crystals. We use the intercrystal phase shift of +28° measured using collimated beams. The resulting calculated values of $\eta(\Delta k_1, \Delta k_2)$ for the two signs of $d_{\text{eff}}$ for the second crystal are shown on the left hand side of Fig. 4. We also show our measured efficiency-surfaces on the right hand side. Our fundamental beam had a nearly Gaussian spatial profile with measured beam quality factor $M^2 = 1.28$ in the walkoff direction and $M^2 = 1.32$ in the orthogonal direction. The measured beam waists were 59 μm in the walkoff direction and 63 μm in the orthogonal direction. These deviations from perfect Gaussian profiles may account for the slight differences between measured and calculated surfaces.

We also measured and calculated conversion efficiency with and without walkoff compensation. Eq. (8) predicts an improvement by a factor of 1.89 with compensation, while we measured an improvement of 1.75.

We next set the crystal orientations to correspond to the peak of the $\eta(\Delta k_1, \Delta k_2)$ surface shown in Fig. 4(b). Tilting the input beam in the walkoff plane away from this point corresponds to moving along a diagonal line parallel to the ridge of highest efficiency. The measured efficiency as a function of the fundamental beam tilt angle is shown as the solid line in Fig. 5. We also show the prediction of Eq. (10) (heavy dashed line) which agrees well with the measurement, and the predictions of Eqs. (4.1)–(4.4) of [3] (light dashed line) which predicts strong modulation of the SH efficiency. The difference in the two predictions is due the inclusion of the extra phase of $iL(\Delta k_1 - \Delta k_2)$ between the contributions from the two crystals in [3]. Ref. [3] reports measuring a curve for type II mixing in RTA with a single peak similar to our measured curve in Fig. 5, rather than the multipeaked behavior predicted by their theory. They explain their result by citing "strong focusing conditions"; however, theories derived using the heuristic method should be valid for their measurement.
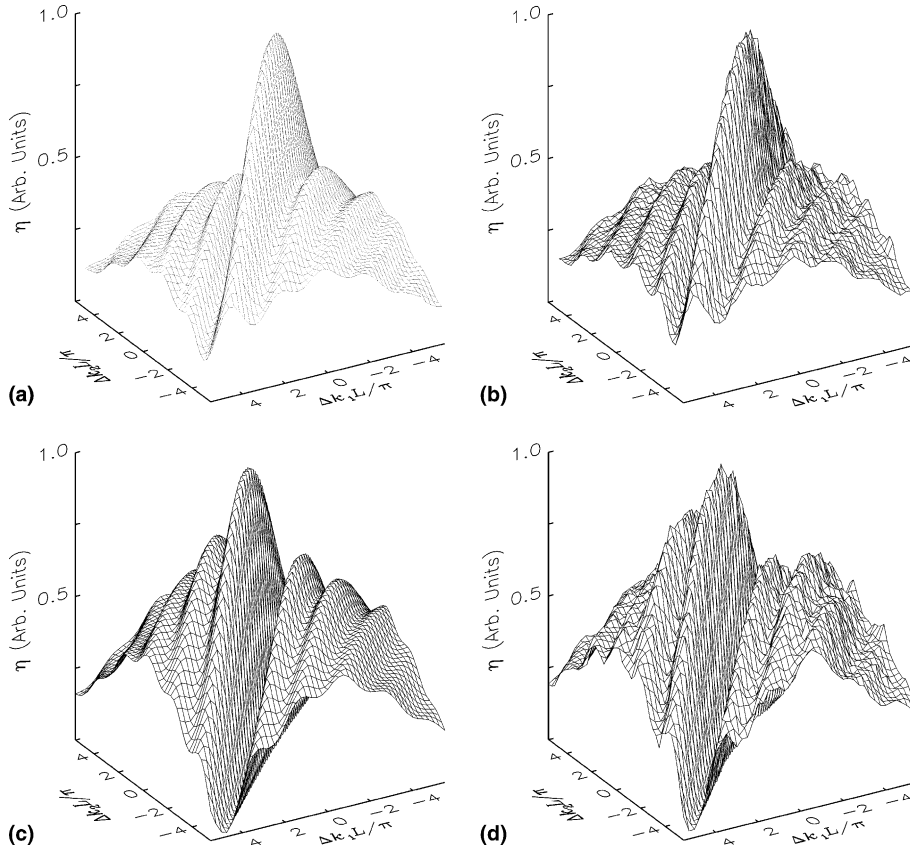
Fig. 4. Second harmonic efficiency surfaces (b and d) measured and (a and c) calculated using Eq. (9). Plots (c) and (d) are for the same orientation of the second crystal as Fig. 3. Plots (a) and (b) are with the second crystal rotated to reverse $d_{eff}$ without changing walkoff. In calculating (c), we use the same intercrystal phase shift ($\Delta\phi = -152°$) that gave the best fit in plane wave case of Fig. 3.

We believe the measurements reported here plus those of [1] show conclusively that the equations in Section 2 correctly describe harmonic generation for two crystals.

### 3.3. Far field fluence patterns for focused beams

As a further check on our theory and as a check on the quality of the beams generated in walkoff-compensated crystals, we also examined the far field SH fluence distributions, comparing calculated and measured profiles. The calculated profiles come from integrating Eq. (8) over $\tau'$ but not over $x$ and $y$. In the limit of $z \to \infty$ we find the distribution as a function of the angles $x/z$ and $y/z$. The measurements are performed as described above except we measure the distributions using a camera placed one focal length away from a focusing lens.

Fig. 6 shows the measured fluence profiles when the crystal tilts are adjusted to lie at several points on the $\eta(\Delta k_1, \Delta k_2)$ surface as indicated by the arrows linking the profiles with points on the surface. The corresponding calculated profiles are shown in Fig. 7. Note that at the point of maximum $\eta(\Delta k_1, \Delta k_2)$ the far field pattern shown in Fig. 6(c) is nearly centered in the forward direction. If the crystals are tilted away from this alignment the pattern is distorted (b) or shifted in angle (a and d).
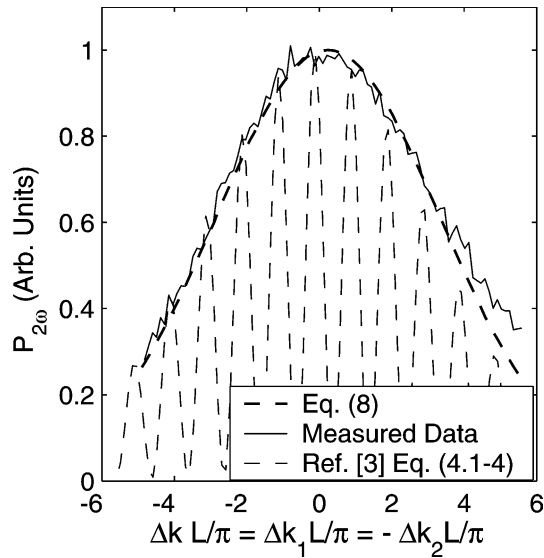
Fig. 5. Comparison of the acceptance angle for focused beams (solid line) measured; (heavy dashed line) according to Eq. (10) of this paper; (light dashed line) according to the theory of [3]. The crystals are oriented to lie at the maximum efficiency point of Figs. 4(a) and (b) and the fundamental beam is tilted to vary the phase mismatch along the ridge of high efficiency. Similar curves to the light dashed line can be found in Figs. 3 and 6 of [3].
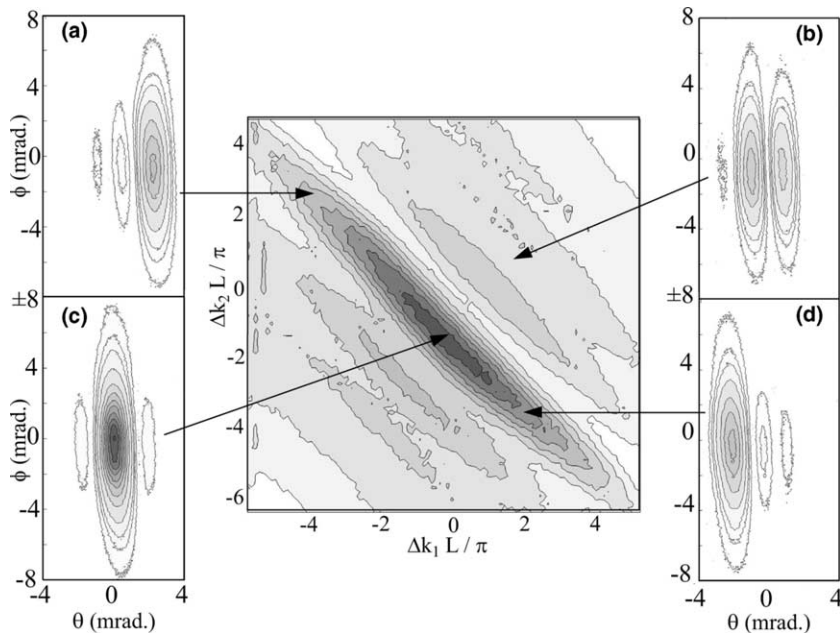


Fig. 6. Measured far field SH fluence patterns for four values of $(\Delta k_1 L/\pi, \Delta k_2 L/\pi)$ indicated by the arrows. The contour lines are evenly spaced except for the three lowest contours which are included to highlight the weak outlying structure.
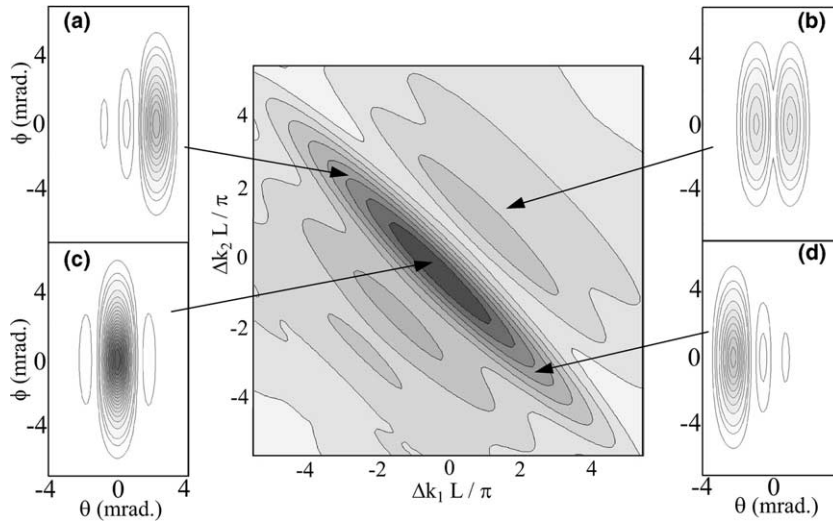
Fig. 7. Calculated far field SH fluence patterns for the same conditions as in Fig. 6.
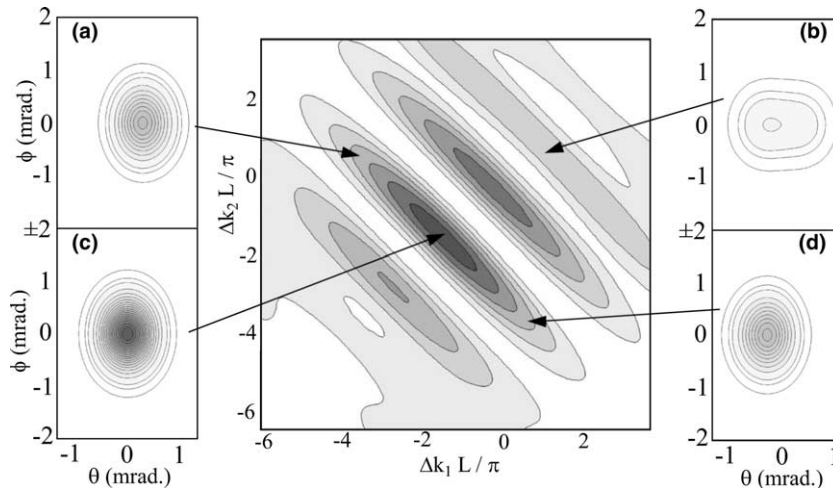


Fig. 8. Calculated far field SH fluence patterns for two 5 mm long, walk-off compensated RTA crystals phase matched for polar-izations (o + e → o), a fundamental beam waist $w_0 = 22$ μm positioned at the junction of the two crystals which are butted together, a fundamental wavelength of $\lambda = 1319$ nm, and a walk off angle of $\rho = 1.3°$. $d_{eff}$ has the same sign for both crystals, and the intercrystal phase shift is 0°.

Finally, we have applied the same theoretical treatment to the case of mixed fundamental polarizations or type II doubling. The resulting $\eta(\Delta k_1, \Delta k_2)$ surface and far field fluence profiles are shown in Fig. 8. Fig. 7.a of [3] shows a highly modulated fluence profile for the same conditions as in Fig. 8 of this paper. However, those data have rather large scatter and error bars. We find that neither the $\eta(\Delta k_1, \Delta k_2)$ surface nor the far field profiles are modulated as was reported in [3] even though the parameters chosen for our simulation correspond to those in [3].

## 4. Summary

We have presented mathematical expressions based on the heuristic method pioneered by Boyd and Kleinman [6] for second harmonic generation in two walkoff-compensated crystals. The predicted surfaces of normalized efficiency as a function of crystal angle, $\eta(\Delta k_1, \Delta k_2)$, are compared with laboratory measurements and shown to be in good agreement. Computed and measured far field SH fluence patterns also match well. Our results underline the two primary benefits of walkoff compensation, increased angular acceptance and increased conversion efficiency without significant beam distortion.

## Acknowledgements

## References

[1] A.V. Smith, D.J. Armstrong, W.J. Alford, J. Opt. Soc. Am. B 15 (1998) 122.
[2] J.-J. Zondy, Opt. Commun. 119 (1995) 320.
[3] J.P. Feve, J.-J. Zondy, B. Boulanger, R. Bonnenberger, X. Cabirol, B. Menaert, G. Marnier, Opt. Commun. 161 (1999) 359.
[4] D.J. Armstrong, W.J. Alford, T.D. Raymond, A.V. Smith, M.S. Bowers, J. Opt. Soc. Am. B 14 (1997) 460.
[5] J.-J. Zondy, M. Abed, S. Khodja, J. Opt. Soc. Am. B 11 (1994) 2368.
[6] G.D. Boyd, D. Kleinman, J. Appl. Phys. 39 (1968) 3597.
[7] D.R. Lide, CRC Handbook of Chemistry and Physics, 81st ed., CRC Press, Boca Raton, 2000.
[8] D. Kleinman, A. Ashkin, G.D. Boyd, Phys. Rev. 145 (1966) 338.